*Int. J. Appl. Math. Comput. Sci., 2018, Vol. 28, No. 2, 349–362*
DOI: 10.2478/amcs-2018-0026

# SIMULTANEOUS DISTURBANCE COMPENSATION AND $H_I/H_\infty$ OPTIMIZATION IN FAULT DETECTION OF UAVs

HAI LIU [a], MAIYING ZHONG [b,*], RUI YANG [b]

[a]Department of Inertia Technology and Navigation Instrumentation
Beihang University, Beijing 100191, China

[b]College of Electrical Engineering and Automation
Shandong University of Science and Technology, Qingdao 266590, China
e-mail: myzhong@buaa.edu.cn

This paper deals with the problem of robust fault detection (FD) for an unmanned aerial vehicle (UAV) flight control system (FCS). A nonlinear model to describe the UAV longitudinal motions is introduced, in which multiple sources of disturbances include wind effects, modeling errors and sensor noises are classified into groups. Then the FD problem is formulated as fault detection filter (FDF) design for a kind of nonlinear discrete time varying systems subject to multiple disturbances. In order to achieve robust FD performance against multiple disturbances, simultaneous disturbance compensation and $H_i/H_\infty$ optimization are carried out in designing the FDF. The optimality of the proposed FDF is shown in detail. Finally, both simulations and real flight data are applied to validate the proposed method. An improvement of FD performance is achieved compared with the conventional $H_i/H_\infty$-FDF.

**Keywords:** fault detection(FD), $H_i/H_\infty$ optimization, disturbance compensation, unmanned aerial vehicle (UAV).

## Nomenclature

| | |
|---|---|
| FD | fault detection |
| FDF | fault detection filter |
| FDI | fault detection and isolation |
| FCS | flight control system |
| UAV | unmanned aerial vehicle |
| INS | inertial navigation system |
| GPS | global positioning system |

## 1. Introduction

UAVs are widely used in both civilian and military applications such as geological exploration, traffic monitoring, border patrol, surveillance and reconnaissance assignments. Because of the economic benefits of UAVs and the key roles they play in modern military applications, tremendous research effort is paid to UAV related techniques (see Cho *et al*., 2011; Péni *et al*., 2015; Pereira *et al*., 2017; Nicotra *et al*., 2017). In most applications of UAVs, the reliability and survivability are of essential interest and have drawn significant attention to FDI techniques. In this paper, the problem of FD of an UAV FCS is investigated.

UAVs are typical nonlinear systems, and when model-based FD is considered, different kinds of disturbances such as sensor noises, modeling errors and wind effects must be taken into account and carefully handled. What is more, sensors on some small UAVs are often limited due to cost and load. Therefore, robust FD of UAVs is definitely a challenging work. Extensive studies about FDI of both manned and unmanned aircrafts have been carried out. In the work of Freeman *et al*. (2013), FD of a certain UAV is accomplished by using both model-based and data-driven methods, and the standard $H_\infty$ formulation is employed for fault estimation. Rosa and Silvestre (2013) applied a linear parameter varying model to describe the UAV dynamic model and the set-valued observer is designed for FDI. In the works of Hajiyev (2013) and Caliskan *et al*. (2014), two-stage Kalman filter based approaches are employed to estimate actuator faults. Bateman *et al*. (2011) apply the unknown input decoupled functional observer to estimate the unknown inputs. In the work of Chabir *et al*.

*Corresponding author

(2014), attitude sensor fault diagnosis of a quadrotor is accomplished with a robust FDF and a novel residual evaluation scheme.

However, all these works have been carried out based on a linearized aircraft model and the proposed methods are usually only valid around the trim condition. If techniques used to achieve a robust performance against intensive model uncertainties are considered, conservative detection performance is inevitable. Therefore, the approaches that can deal with nonlinear models directly are required.

In the works of Ducard and Geering (2008) as well as Lu *et al*. (2015), a multi-model adaptive estimation approach is employed to make FDI function with nonlinear aircraft models. In these works, disturbances and noises are assumed to be stochastic signals with known statistical properties. Cen *et al*. (2015) employ two Thau observers to detect and estimate the fault of a quadrotor. In work of Wu *et al*. (2015), several nonlinear estimation methods are proposed for the purpose of fault diagnosis of an unmanned helicopter and a comparative study is carried out. It should be noted that the norm bounded assumption of disturbance is more appropriate when disturbance such as wind and model uncertainties are considered. In these studies, robust diagnosis performance against the disturbance is not the main concern.

Rodriguez-Alfaro *et al*. (2015) propose a Hamiltonian approach to fault isolation for a type of UAV. This kind of fault isolation method is limited to a special kind of systems. More works on FDI for FCS include those by Henry *et al*. (2015) and Lu *et al*. (2016). However, these approaches cannot be directly used because the sensors available on the low-cost UAVs are limited. Meanwhile, as stated by Lu *et al*. (2016), the presence of time-varying wind and turbulence is one of the biggest challenges for FDI of FCS, and it has not been seriously treated in the existing works. Specifically, wind effects will either lead to false alarms when the threshold is set too low, or cause many faults undetectable when the threshold is set too high. Therefore, a new FD method that can deal with nonlinearity and multiple norm bounded disturbances, and lead to less conservative result is desired.

On the other hand, there have been significant research activities devoted to design and analysis of FDI methods in recent years; see the works of Ding (2013), Hassanabadi *et al*. (2016), Zhong *et al.* (2016a; 2017), Xu *et al*. (2017), Zhao and Huang (2017), and the references therein. Among the developed FDI theories, FDF based FD proves to be one of the most effective methods. The well-known $H_\infty/H_\infty$ and/or $H_-/H_\infty$ optimization is widely adopted in FDF design such that robust performance is achieved in the sense that a sensitivity/robustness ratio is maximized. When linear systems are considered, remarkable results are achieved, (see Ding *et al.*, 2000; Zhong *et al.*, 2010; 2016a; Li *et al.*, 2015). In contrast to the linear case, works about optimal FD for nonlinear systems are relatively limited.

In the work of Khan *et al*. (2014), $H_-/H_\infty$-FDF for a kind of discrete time nonlinear systems is proposed with the help of a zero sum differential game. Boulkroune *et al*. (2013) proposed robust FDF design in the $H_-/H_\infty$ framework for a kind of nonlinear descriptor systems as a convex optimization problem solved via linear matrix inequality techniques. In the authors' previous work (Zhong *et al*., 2015), an extended $H_-/H_\infty$ solution in a recursive form is obtained for a kind of nonlinear discrete time systems, and its application to FD of an INS/GPS integrated system is shown by Zhong *et al*. (2016b). However, the optimality of the proposed FDF is not shown clearly for the nonlinear case. Though $H_-/H_\infty$ optimization can be considered in FDF design for UAVs, the FD performance can be still conservative because of the wind effects.

Wind estimation techniques get a lot of attention in fields such as aircraft guidance, control, trajectory prediction and so on; see the works of Mulgund and Stengels (1996), Tanaka and Suzuki (2006), Langelaan *et al*. (2011), Lee *et al*. (2014), and the references therein. Generally, the existing wind estimation techniques can be divided into two categories: one is a graphical method and the other is an observer based method. In the graphical method, adequate sensors include GPS, INS, and air data system are usually needed to compute the wind speed. Thus, the observer based method is much more attractive. In fact, a disturbance observer is widely used in controller and observer design to achieve disturbance rejection performance. In the work of Guo and Cao (2014) and the references therein, a hierarchical anti-disturbance framework is proposed in which the disturbance observer is incorporated with different control methods and thus multiple sources of disturbances are handled in different ways to achieve nonconservative results. Inspired from this, an FDF in which wind effects compensation and $H_i/H_\infty$ optimization are carried out simultaneously, is proposed for robust FD of UAVs. This is the basic idea of this paper. Here the name $H_i/H_\infty$ optimization is adopted because both $H_\infty/H_\infty$ and $H_-/H_\infty$ optimization problems are treated with a unified solution in this study.

Compared with the authors' previous works (Zhong *et al.*, 2010; 2015), contributions of this paper lie in two aspects. First, multiple disturbances are considered and classified into different groups. Then simultaneous disturbance compensation and $H_i/H_\infty$ carried out in FDF design. Thus an improved detection performance is achieved. Second, as a nonlinear system is considered, the optimality of the proposed FDF is shown in a new and more rigorous way when compared with the previous

work (Zhong *et al*., 2015).

The paper is organized as follows. The FD problem of the UAV FCS is analyzed and formulated in Section 2. Section 3 is dedicated to FDF design. In Section 4, both simulations and real flight data are utilized to validate the proposed method Conclusions is are included in Section 5.

**Notation.** For a vector $z(k)$ we define

$$\|z(k)\|_2^2 = z^T(k)z(k)$$

and

$$\|z(k)\|_{R^{-1}}^2 = z^T(k)R^{-1}z(k).$$

Here $z(k) \in l_2[0, N]$ means

$$\sum_{k=0}^{N} z^T(k)z(k) < \infty$$

and for a sequence $\{z(k)\}_{k=0}^N$,

$$z_N = [z^T(0) \quad z^T(1) \quad \cdots \quad z^T(N)]^T$$

is adopted. $\|M\|_2$ and $\|M\|_-$ denote the largest and smallest singular value of matrix $M$, respectively. For a nonlinear mapping $\mathcal{M}$ such that $y_N = \mathcal{M}u_N$, the $H_\infty$ norm and the $H_-$ index of the nonlinear mapping are defined as

$$\|\mathcal{M}\|_\infty = \sup_{u_N \neq 0} \frac{\sum\limits_{k=0}^{N} \|y(k)\|_2}{\sum\limits_{k=0}^{N} \|u(k)\|_2},$$

$$\|\mathcal{M}\|_- = \inf_{u_N \neq 0} \frac{\sum\limits_{k=0}^{N} \|y(k)\|_2}{\sum\limits_{k=0}^{N} \|u(k)\|_2},$$

respectively. $\mathcal{M}_a \circ \mathcal{M}_b$ indicates two compatible mappings, i.e., the outputs of $\mathcal{M}_b$ are the inputs of $\mathcal{M}_a$.

## 2. UAV model and problem formulation

**2.1. Faulty UAV model for FDF design.** In this section, a faulty UAV model with multiple sources of disturbances is established in the state space form for FDF design. According to the coupling of different motions, the equations to describe the dynamic/kinetic of UAV can be grouped into the longitudinal model and the lateral model. This decoupling is widely adopted and results in an easier system analysis and controller/observer design (see Rosa and Silvestre, 2013; Hajiyev, 2013; Freeman *et al*., 2013; Caliskan *et al*., 2014; Péni *et al*., 2015). In this study, FDF design for the longitudinal UAV model is considered. It should be noted that model decoupling is a restrictive assumption for the case of large amplitude lateral maneuvering such as a coordinated turn. False alarms are inevitable in such a case and must be carefully treated. Nevertheless, during a considerable time period of flight, lateral motions are mild, and false alarms triggered by lateral maneuvering can be recognized by means of the control law. Thus, it is reasonable to use the longitudinal model for design.

A three degree-of-freedom model taking account of wind effects, which is introduced after Frost and Bowles (1984), is as follows:

$$\begin{cases} \dot{V} = \dfrac{1}{m}(P\cos\alpha - D - mg\sin(\theta-\alpha)) \\ \qquad -\dot{W}_x\cos(\theta-\alpha) - \dot{W}_z\sin(\theta-\alpha), \\ \dot{\alpha} = \dfrac{1}{mV}(-L + P\sin\alpha + mg\cos(\theta-\alpha)) + q \\ \qquad -\dot{W}_x\dfrac{\sin(\theta-\alpha)}{V} + \dot{W}_z\dfrac{\cos(\theta-\alpha)}{V}, \\ \dot{q} = \dfrac{M_y}{I_y}, \\ \dot{\theta} = q, \\ \dot{H} = V\sin(\theta-\alpha) + W_z, \end{cases}$$

where forces and the moment are formulated as

$$P = K\delta_p, \qquad D = \bar{q}S_wC_x,$$
$$L = \bar{q}S_wC_y \qquad M_y = \bar{q}S_w\bar{c}C_m$$

with

$$\bar{q} = \frac{\rho V^2}{2},$$
$$C_x = C_{x0} + C_x^\alpha\alpha + C_x^{\alpha^2}\alpha^2,$$
$$C_y = C_{y0} + \frac{\bar{c}C_y^q}{2V}q + C_y^{\delta_e}\delta_e,$$
$$C_m = C_{m0} + \frac{\bar{c}C_m^q}{2V}q + m_y^{\delta_e}\delta_e.$$

In the above model, state variables $V$, $\alpha$, $q$, $\theta$, and $H$ denote the air speed, the angle of attack, the pitch rate, the pitch angle and the altitude, respectively. Here $\delta_e$ is the elevator deflection and $\delta_p$ is the throttle setting. $W_z$ is the wind speed in the vertical direction and $\dot{W}_x$, $\dot{W}_z$ are wind gradients in the horizontal and vertical directions, respectively. Parameters $g$, $\rho$, $m$, $I_y$, $S_w$, $\bar{c}$ represent the gravitational constant, air density, UAV mass, inertia, reference area and mean aerodynamic chord, respectively. $K$ is engine thrust coefficient and $C_{x0}$, $C_x^\alpha$, $C_x^{\alpha^2}$, $C_{y0}$, $C_y^q$, $m_{y0}$, $m_y^q$, $C_y^{\delta_e}$, $m_y^{\delta_e}$ are all aerodynamic coefficients obtained from a wind tunnel test.

Actuators and sensors are fundamental equipment in FCS. Sensors are employed to provide measurement feedback, while actuators provide propulsion and incremental forces to ensure that the desired attitude and speed of the UAV are achieved. Faults of actuators or

sensors are inevitable and may lead to disasters for UAV systems. Typical actuator faults include a loss of control effectiveness, and unwanted oscillations, deflection, a jamming of the control surface, and common sensor faults are reflected by a bias or a drift in sensors' outputs. According to Ding (2013, Section 3.5), these actuator and sensor faults can be modeled as additive faults for the purpose of FD.

Set the control inputs $u(t) = [\delta_e \quad \delta_p]^T$, the measurements $y(t) = [V_m \quad \theta_m \quad q_m \quad H_m]$, the state vector $x(t) = [V \quad \alpha \quad q \quad \theta \quad H]^T$, the disturbance vector $d(t) = [W_z \quad \dot{W}_x \quad \dot{W}_z]^T$. The following state space model is obtained:

$$\begin{cases} \dot{x}(t) = F(x(t)) + B(x(t))u(t) + B_d(x(t))d(t) \\ \qquad\quad +B_w(x(t))w(t) + B_f(x(t))f(t), \\ y(t) = Cx(t) + v(t) + D_f(t)f(t), \end{cases} \tag{1}$$

where $f(t)$ is the fault, $w(t)$ is an artificial signal employed to represent modeling errors and $v(t)$ is the measurement noise. Here $w(t)$ and $v(t)$ are also energy bounded, and the covariance $R$ of $v(t)$ is assumed known. In the above state space model,

$$F(x(t)) = \begin{pmatrix} \Big( -\dfrac{\rho V^2 S_w}{2m}(C_{x0} + C_x^{\alpha}\alpha + C_x^{\alpha^2}\alpha^2) \\ \qquad -g\sin(\theta-\alpha)\Big) \\ -\dfrac{\rho V S_w}{2m}(C_{y0} + \dfrac{C_y^q \bar{c}}{2V}q) + \dfrac{g}{V}\cos(\theta-\alpha) + q \\ \dfrac{\rho V^2 S_w \bar{c}}{2I_y}(m_{y0} + \dfrac{m_y^q \bar{c}}{2V}q) \\ q \\ V\sin(\theta-\alpha) \end{pmatrix},$$

$$C = \begin{pmatrix} 1 & 0 & 0 & 0 & 0 \\ 0 & 0 & 1 & 0 & 0 \\ 0 & 0 & 0 & 1 & 0 \\ 0 & 0 & 0 & 0 & 1 \end{pmatrix},$$

$$B(x(t)) = \begin{pmatrix} 0 & \dfrac{K\cos\alpha}{m} \\ -\dfrac{\rho V S_w C_y^{\delta_e}}{2m} & \dfrac{K\sin\alpha}{mV} \\ \dfrac{\rho V^2 S_w \bar{c} m_y^{\delta_e}}{2I_y} & 0 \\ 0 & 0 \\ 0 & 0 \end{pmatrix},$$

$$B_d(x(t)) = \begin{pmatrix} 0 & -\cos(\theta-\alpha) & -\sin(\theta-\alpha) \\ 0 & -\dfrac{\sin(\theta-\alpha)}{V} & \dfrac{\cos(\theta-\alpha)}{V} \\ 0 & 0 & 0 \\ 0 & 0 & 0 \\ 1 & 0 & 0 \end{pmatrix}.$$

Because of the uncertainties in aerodynamic coefficients and model decoupling, variations in aerodynamic forces $D$, $L$ and moment $M_y$ from their nominal values are inevitable. These uncertainties are the main modeling errors and $B_w(x(t))$ is chosen as

$$B_w(x(t)) = \begin{bmatrix} 1 & 0 & 0 & 0 & 0 \\ 0 & 1 & 0 & 0 & 0 \\ 0 & 0 & 1 & 0 & 0 \end{bmatrix}^T.$$

Finally, $B_f(x(t))$ and $D_f(x(t))$ are determined by the fault that occurs. For example, when an elevator fault occurs, we have

$$B_f(x(t)) = \begin{bmatrix} 0 & -\frac{\rho V S_w C_y^{\delta_e}}{2m} & \frac{\rho V^2 S_w \bar{c} m_y^{\delta_e}}{2I_y} & 0 & 0 \end{bmatrix}^T,$$

$$D_f(t) = \mathbf{0},$$

and a pitot fault is described as

$$B_f(x(t)) = \mathbf{0}, \quad D_f(t) = \begin{bmatrix} 1 & 0 & 0 & 0 \end{bmatrix}^T.$$

Note that in the state space model (1), the wind disturbance $d(t)$ can affect the detection performance seriously, and in the mean time, $d(t)$ enters the UAV system in a different way from actuator and sensor faults. Thus, wind estimation and compensation is required in designing the FDF. On the contrary, compensation of $w(t)$ is undesirable because both modeling errors $w(t)$ and actuator faults result in variations in aerodynamic forces or moment. The compensation of $w(t)$ leads to the compensation of faults, which makes FD performance even worse. Meanwhile, it should be noted that modeling errors and wind disturbances may affect the designed FDF in a more complicated way in real applications. A perfect discrimination of their effects is scarcely possible. In this study, FD of a UAV in a gusty condition is considered. To minimize the effect of multiple disturbances on the FDF, modeling errors and wind disturbances are treated differently.

Motion of the air shows highly nonlinear and even chaotic behaviors. Thus, physical modeling of wind dynamics is still an open problem. Fortunately, wind estimation is still available by using a constant wind model or a polynomial model due to the fact that the gust wind can be interpreted as a superposition of the turbulence on the low frequency dominant wind (see Mulgund and Stengels, 1996; Tanaka and Suzuki, 2006; Cho *et al.*, 2011). In this study, two-order polynomials

are adopted and the wind dynamics used for disturbance estimation is expressed as

$$\begin{cases} \dot{\zeta}(t) = A_\zeta \zeta(t) + B_\zeta \varepsilon(t), \\ d(t) = C_\zeta \zeta(t), \end{cases} \tag{2}$$

where $\zeta(t) = [W_x \quad W_z \quad \dot{W}_x \quad \dot{W}_z]^T$, $\varepsilon(t)$ is energy bounded and supposed to include external perturbations and model uncertainties for the wind dynamics, and

$$A_\zeta = \begin{bmatrix} 0 & I_2 \\ 0 & 0 \end{bmatrix}, \quad B_\zeta = \begin{bmatrix} 0 \\ I_2 \end{bmatrix}, \quad C_\zeta = \begin{bmatrix} 0 & I_3 \end{bmatrix}.$$

**2.2. Problem formulation.** Euler discretization is employed and the following nonlinear discrete time UAV model is obtained:

$$\begin{cases} x(k+1) = \mathcal{A}(x(k)) + \mathcal{B}(x(k))u(k) \\ \qquad\qquad +\mathcal{B}_d(x(k))d(k) + \mathcal{B}_w(x(k))w(k) \\ \qquad\qquad +\mathcal{B}_f(x(k))f(k), \\ y(k) = Cx(k) + v(k) + D_f(k)f(k), \end{cases} \tag{3}$$

where

$$\begin{aligned} \mathcal{A}(x(k)) &= T_s F(x(k)) + x(k), \\ \mathcal{B}(x(k)) &= T_s B(x(k)), \\ \mathcal{B}_d(x(k)) &= T_s B_d(x(k), \\ \mathcal{B}_f(x(k)) &= T_s B_f(x(k). \end{aligned}$$

Similarly, discretization of wind dynamics (2) is obtained as follows:

$$\begin{cases} \zeta(k+1) = A_e \zeta(k) + B_e \varepsilon(k), \\ d(k) = C_e \zeta(k) \end{cases} \tag{4}$$

where $A_e = I + T_s A_\zeta$, $B_e = T_s B_\zeta$, $C_e = C_\zeta$. Then the FD problem of the UAV FCS is formulated as follows:

Consider a class of nonlinear discrete-time systems with multiple disturbances described in (3), where $x(k)$, $u(k)$, $y(k)$, $f(k)$ are the state, the control inputs, the outputs and the fault, respectively. The considered multiple disturbances, $d(k)$, $w(k)$ and $v(k)$, are $l_2[0, N]$-norm bounded. Furthermore, the covariance $R$ of $v(k)$ is assumed to be known. Thus $\sum_0^N \|v(k)\|^2_{R^{-1}}$ is also bounded. Here $d(k)$ is supposed to be described by the exogenous system (4), where $\zeta(k)$ is the state of the exogenous system and $\varepsilon(k)$ is also the $l_2[0, N]$-norm. $A_e$, $B_e$ and $C_e$ are known constant matrices with appropriate dimensions. In the nonlinear system (3), $\mathcal{A}$, $\mathcal{B}$, $\mathcal{B}_d$, $\mathcal{B}_w$ and $\mathcal{B}_f$ are smooth functions with respect to $x(k)$. Furthermore, it is assumed that

$$\mathrm{Im}(\mathcal{B}_f(x(k))) \subset \mathrm{Im}(\mathcal{B}_w(x(k))), \tag{5}$$

$$\mathrm{Im}(\mathcal{B}_f(x(k))) \cap \mathrm{Im}(\mathcal{B}_d(x(k))) = \mathbf{0}. \tag{6}$$

The former assumption (5) is quite standard in $H_i/H_\infty$-FDF design (see Ding *et al.*, 2000). Here (6) is used to guarantee that the fault $f(k)$ is not estimated and compensated as the disturbance $d(k)$. Physically, (6) implies that the fault and disturbances affect the system with different distribution matrices, and the columns of these two matrices are linearly independent. Though this assumption seems restrictive, it is reasonable to select part of the disturbances such that (6) is fulfilled, while other disturbances are classified as $w(t)$. Furthermore, it should be noted that estimation and compensation is a solution to reduce the influence of disturbance, but FD performance is still affected.

Since it is desired that estimation and compensation of $d(k)$ are integrated into $H_i/H_\infty$ optimization, the following observer based nonlinear FDF is proposed:

$$\begin{cases} \hat{x}(k+1) = \mathcal{A}(\hat{x}(k)) + \mathcal{B}(\hat{x}(k))u(k) \\ \qquad\qquad +\mathcal{B}_d(\hat{x}(k))\hat{d}(k) + K(k)\tilde{y}(k), \\ \hat{\zeta}(k+1) = A_e\hat{\zeta}(k) + L(k)\tilde{y}(k), \\ \hat{d}(k) = C_e\hat{\zeta}(k), \\ \tilde{y}(k) = y(k) - C\hat{x}(k), \\ r(k) = W(k)\tilde{y}(k), \\ \hat{x}(0) = \hat{x}_0, \\ \hat{\zeta}(0) = 0, \end{cases} \tag{7}$$

where the hat stands for an estimated variable, $\tilde{y}(k)$ is the output estimation error and $r(k)$ is the residual.

Introduce $\|G_{rw}\|^2_{\infty,[0,N]}$ to represent the robustness of the residual to unknown inputs, and $\|G_{rf}\|^2_{\infty,[0,N]}$, $\|G_{rf}\|^2_{-,[0,N]}$ to represent the best and worst case sensitivities of residual to fault, respectively. Specifically,

$$\|G_{rw}\|^2_{\infty,[0,N]} = \sup_{f=0} \frac{\sum_{k=0}^{N} \|r(k)\|^2}{\|\tilde{x}_0\|^2 + \sum_{k=0}^{N} (\|w(k)\|^2 + \|\varepsilon(k)\|^2 + \|v(k)\|^2_{R^{-1}})},$$

$$\|G_{rf}\|^2_{\infty,[0,N]} = \sup_{\tilde{x}_0,d,w,v=0} \frac{\sum_{k=0}^{N} \|r(k)\|^2}{\sum_{k=0}^{N} \|f(k)\|^2},$$

$$\|G_{rf}\|^2_{-,[0,N]} = \inf_{\tilde{x}_0,d,w,v=0} \frac{\sum_{k=0}^{N} \|r(k)\|^2}{\sum_{k=0}^{N} \|f(k)\|^2}.$$

Then the problem can be formulated as finding observer gains $K(k)$, $L(k)$, and a postfilter $W(k)$ to solve the

following optimization problems:

$$\max_{K(k),L(k),W(k)} \frac{\|G_{rf}\|^2_{\infty,[0,N]}}{\|G_{rw}\|^2_{\infty,[0,N]}}, \tag{8}$$

$$\max_{K(k),L(k),W(k)} \frac{\|G_{rf}\|^2_{-,[0,N]}}{\|G_{rw}\|^2_{\infty,[0,N]}}. \tag{9}$$

The second stage of FD is residual evaluation. Under the assumption that

$$\|\tilde{x}_0\|^2 + \sum_{k=0}^{N}(\|w(k)\|^2 + \|\varepsilon(k)\|^2 + \|v(k)\|^2_{R^{-1}}) \leq \delta^2 \tag{10}$$

the following residual evaluation function $J_N(k)$ with a sliding window and its threshold $J_{th}$ is adopted:

$$J_N(k) = \frac{1}{N+1}\sum_{j=k-N}^{k} r^T(j)r(j), \tag{11}$$

$$J_{th} = \frac{1}{N+1}\|G_{rw}\|^2_{\infty,[0,N]}\delta^2, \tag{12}$$

and the fault detection logic is specified as

$$\begin{cases} \text{if } J_N(k) \leq J_{th}, & \text{fault free,} \\ \text{if } J_N(k) > J_{th}, & \text{fault alarm.} \end{cases} \tag{13}$$

**Remark 1.** Equation (10) is an assumption about the norm bounded disturbance that is widely adopted in studies on FDF design (Zhong *et al.*, 2010; 2016a; Ding, 2013). As shown in (12), this assumption is used to determine the threshold. Actually, it is very difficult to obtain an analytical value of $\delta$ in real applications. However, an estimate from the historical data is available. In Proposition 4 of Zhong *et al*. (2017), the estimation of $\delta$ and the threshold setting are given in detail.

**Remark 2.** As presented by Ding *et al*. (2000), a fault $f(k)$ can be detected for all possible $w(k)$, $\varepsilon(k)$ and $v(k)$ if

$$\|G_{rf}\|^2_{-,[0,N]}\sum_{k=0}^{N}\|f(k)\|^2 > 2J_{th}.$$

Thus $f(k)$ is said to be strongly detectable if

$$\sum_{k=0}^{N}\|f(k)\|^2 > \frac{2J_{th}}{\|G_{rf}\|^2_{-,[0,N]}}.$$

However, as a nonlinear system is considered, $\|G_{rf}\|^2_{-,[0,N]}$ is very difficult to be identified. Only estimation under specific working conditions is available. More details about the detectability of a fault can be found in Section 3 of the work of Ding *et al*. (2000).

Furthermore, false alarms and missed alarms are inevitable in applications due to the influence of the disturbance and the selection of the threshold. As presented by Ding (2013), an effective way is to set a counter. Specifically, a fault is declared at the step $j_a$ defined as follows.

$$j_a = \min\Big\{j : \sum_{j=k-N}^{k}\text{Alarm}(j) \geq \eta\Big\}, \tag{14}$$

where

$$\text{Alarm}(j) = \begin{cases} 1, & J_N(j) > J_{th}, \\ 0, & J_N(j) \leq J_{th}, \end{cases}$$

and $\eta$ is a predefined number.

## 3. Integrated disturbance compensation and $H_i/H_\infty$ optimization in FDF design

In order to deal with the nonlinearity, a similar procedure proposed in our previous work (Zhong *et al*., 2015) is adopted. The following Taylor expansions can be obtained:

$$\begin{aligned} &\mathcal{A}(x(k)) + \mathcal{B}(x(k))u(k) \\ &\quad = \mathcal{A}(\hat{x}(k)) + \mathcal{B}(\hat{x}(k))u(k) \\ &\qquad + A(k)(x(k) - \hat{x}(k)) + \ldots, \\ &\mathcal{B}_d(x(k)) = B_d(k) + \ldots, \\ &\mathcal{B}_f(x(k)) = B_f(k) + \ldots, \\ &\mathcal{B}_w(x(k)) = B_w(k) + \ldots, \end{aligned}$$

where

$$A(k) = \frac{\partial}{\partial x(k)}(\mathcal{A}(x(k)) + \mathcal{B}(x(k))u(k))\Big|_{x(k)=\hat{x}(k)}, \tag{15}$$

$$B_d(k) = \mathcal{B}_d(\hat{x}(k)), \tag{16}$$

$$B_f(k) = \mathcal{B}_f(\hat{x}(k)), \tag{17}$$

$$B_w(k) = \mathcal{B}_w(\hat{x}(k)). \tag{18}$$

Neglecting the higher order terms yields

$$\begin{aligned} \mathcal{A}(x(k)) + \mathcal{B}(x(k))u(k) &\approx \mathcal{A}(\hat{x}(k)) + \mathcal{B}(\hat{x}(k))u(k) \\ &\quad + A(k)(x(k) - \hat{x}(k)), \\ \mathcal{B}_d(x(k)) &\approx B_d(k), \\ \mathcal{B}_f(x(k)) &\approx B_f(k), \\ \mathcal{B}_w(x(k)) &\approx B_w(k). \end{aligned}$$

With the above approximations, when the nonlinear FDF (7) is employed, it is expected that the observer gains

and the postfilter are selected to solve the optimization problems (8) and (9) approximately. Define

$$\tilde{x}(k) = x(k) - \hat{x}(k),$$
$$\tilde{d}(k) = d(k) - \hat{d}(k),$$
$$\tilde{\zeta}(k) = \zeta(k) - \hat{\zeta}(k),$$
$$s(k) = \begin{pmatrix} \tilde{x}^T(k) & \tilde{\zeta}^T(k) \end{pmatrix}^T,$$
$$\bar{w}(k) = \begin{pmatrix} w^T(k) & \varepsilon^T(k) & v^T(k)R^{-1/2} \end{pmatrix}^T.$$

The following error dynamic system can be obtained:

$$\begin{cases} s(k+1) = \bar{A}_K(k)s(k) + \bar{B}_{Kw}(k)\bar{w}(k) \\ \qquad\qquad +\bar{B}_{Kf}(k)f(k), \\ \tilde{y}(k) = \bar{C}(k)s(k) + \bar{D}_w(k)\bar{w}(k) + D_f(k)f(k), \\ r(k) = W(k)\tilde{y}(k), \end{cases} \tag{19}$$

where

$$\bar{A}_K(k) = \bar{A}(k) - \bar{K}(k)\bar{C}(k),$$
$$\bar{B}_{Kw}(k) = \bar{B}_w(k) - \bar{K}(k)D_w(k),$$
$$\bar{B}_{Kf}(k) = \bar{B}_f(k) - \bar{K}(k)D_f(k),$$

with

$$\bar{A}(k) = \begin{bmatrix} A(k) & B_d(k)C_e \\ 0 & A_e \end{bmatrix}, \tag{20}$$
$$\bar{C}(k) = \begin{bmatrix} C(k) & 0 \end{bmatrix}, \tag{21}$$
$$\bar{K}(k) = \begin{bmatrix} K^T(k) & L^T(k) \end{bmatrix}^T, \tag{22}$$
$$\bar{B}_w(k) = \begin{bmatrix} B_w(k) & 0 & 0 \\ 0 & B_e & 0 \end{bmatrix}, \tag{23}$$
$$\bar{D}_w(k) = \begin{bmatrix} 0 & 0 & R^{1/2} \end{bmatrix}, \tag{24}$$
$$\bar{B}_f(k) = \begin{bmatrix} B_f^T(k) & 0 \end{bmatrix}^T. \tag{25}$$

Note that (19) is a linear discrete time varying system. It is a straightforward idea that solutions of $\bar{K}_o(k)$ and $W_o(k)$ presented by Zhong *et al*. (2010) may solve the optimization problems (8) and (9) approximately. Specifically,

$$\begin{cases} \bar{K}_o(k) = (\bar{A}(k)P_o(k)\bar{C}^T(k) \\ \qquad\qquad +\bar{B}_w(k)\bar{D}_w^T(k))R_{\tilde{y}}^{-1}(k), \\ W_o(k) = R_{\tilde{y}}^{-1/2}(k), \\ R_{\tilde{y}}(k) = \bar{C}(k)P_o(k)\bar{C}^T(k) + \bar{D}_w(k)\bar{D}_w^T(k), \\ P_o(k+1) = \bar{A}(k)P_o(k)\bar{A}^T(k) + \bar{B}_w(k)\bar{B}_w^T(k) \\ \qquad\qquad -\bar{K}_o(k)R_{\tilde{y}}(k)\bar{K}_o^T(k), \\ P_o(0) = I. \end{cases} \tag{26}$$

The proof of optimality for the linear case is presented by Zhong *et al*. (2010) and, roughly, it can be divided into three stages:

*Stage 1*: Show $\|G_{rw,o}\|^2_{\infty,[0,N]} = 1$ when $\bar{K}_o(k)$ and $W_o(k)$ in (26) is applied.

*Stage 2*: The observer gain $\bar{K}_o(k)$ and the post filter $W_o(k)$ are replaced with arbitrary $\bar{K}_a(k)$ and $W_a(k)$, respectively, which still keep the FDF stable. Show that there exist a mapping such that the new residual $r_{N,a}$ can be recovered from the optimal residual $r_{N,o}$, i.e., $r_{N,a} = H_{rro}r_{N,o}$.

*Stage 3*: Denoting $r_{N,a} = H_{rw}\bar{w}_N + H_{rf}f_N$ and $r_{N,o} = H_{rw,o}\bar{w}_N + H_{rf,o}f_N$, show that

$$\frac{\|H_{rf}\|_i^2}{\|H_{rw}\|_2^2} = \frac{\|H_{rro}\cdot H_{rf,o}\|_i^2}{\|H_{rro}\cdot H_{rw,o}\|_2^2} \le \frac{\|H_{rf,o}\|_i^2}{\|H_{rw,o}\|_2^2}.$$

To achieve the goal in *Stage 2* by Zhong *et al*. (2010) it is shown that $\tilde{y}_a(k)$ obtained with the new observer gain $\bar{K}_a(k)$ can be recovered by the following system, which is driven by $\tilde{y}_o(k)$:

$$\begin{cases} \eta(k+1) = (\bar{A}(k) - \bar{K}_a(k)\bar{C}(k))\eta(k) \\ \qquad\qquad +(\bar{K}_o(k) - \bar{K}_a(k))\tilde{y}_o(k), \\ \tilde{y}_a(k) = \bar{C}(k)\eta(k) + \tilde{y}_o(k), \\ \eta(0) = 0. \end{cases} \tag{27}$$

However, in this study, it is observed that $\bar{K}_o(k)$ and $\bar{K}_a(k)$ will lead to different Jacobian matrices and, therefore, $\bar{A}(k)$ in (27) is undefined, while for the linear case considered by Zhong *et al*. (2010) system matrices are predefined. This subtle difference makes it inappropriate to use (27) again. A new mapping between $\tilde{y}_{N,a}$ and $\tilde{y}_{N,o}$ must be constructed. In the following, these three stages to prove the optimality are shown in a new and more rigorous way.

*Stage 1*: Define

$$\Phi(j,i) = \prod_{k=i}^{j-1} \bar{A}_K(k),$$
$$\Phi(j,j) = I.$$

Then (19) can be rewritten as

$$\tilde{y}_N = \Omega s(0) + \Gamma_w\bar{w}_N + \Gamma_f f_N$$

and

$$r_N = W_N\tilde{y}_N,$$

where

$$\Omega = \begin{bmatrix} \bar{C}(0) \\ \bar{C}(1)\Phi(1,0) \\ \vdots \\ \bar{C}(N)\Phi(N,0) \end{bmatrix},$$
$$\Gamma_w = \begin{bmatrix} \Gamma_w(k,j) \end{bmatrix}_{(N+1)\times(N+1)},$$
$$W_N = \operatorname{diag}\begin{pmatrix} W(0) & W(1) & \cdots & W(N) \end{pmatrix},$$

$$\Gamma_w(k,k) = \bar{D}_w(k),$$

$$\Gamma_w(k,j) = \begin{cases} 0 & \text{for} \quad k < j, \\ \bar{C}(k)\Phi(k-1,j)\bar{B}_{K,w}(j) & \text{for} \quad k > j, \end{cases}$$

and $\Gamma_f$ is constructed by replacing $\{\bar{B}_w(k), \bar{D}_w(k)\}$ in $\Gamma_w$ with $\{\bar{B}_f(k), D_f(k)\}$. Then it can be shown that

$$\|G_{rw}\|^2_{\infty,[0,N]} = \left\| \begin{array}{cc} W_N[\Omega & \Gamma_w] \end{array} \right\|_2^2.$$

The following linear stochastic system is introduced:

$$\begin{cases} \mathbf{s}(k+1) = \bar{A}_K(k)\mathbf{s}(k) + \bar{B}_{Kw}(k)\bar{\mathbf{w}}(k), \\ \tilde{\mathbf{y}}(k) = \bar{C}(k)\mathbf{s}(k) + \bar{D}_w(k)\bar{\mathbf{w}}(k), \end{cases}$$

where $\mathbf{s}(0)$ and $\bar{\mathbf{w}}(k)$ are assumed to be white noise with zeros mean and unit covariance

$$E\left( \begin{bmatrix} \mathbf{s}(0) \\ \bar{\mathbf{w}}(i) \end{bmatrix} \begin{bmatrix} \mathbf{s}^T(0) & \bar{\mathbf{w}}^T(j) \end{bmatrix} \right) = \begin{bmatrix} I & 0 \\ 0 & \delta_{ij} I \end{bmatrix},$$

where $\delta_{ij}$ is the Kronecker-delta function. Then it is obvious that $\bar{K}_o(k)$ defined in (26) becomes the solution of the well-known Kalman filter. Specifically, $P_o(k)$ and $R_{\tilde{y}}(k)$ are covariances of the state estimation error and the innovation, respectively. Then the orthogonality of the innovation sequences yields

$$E\begin{pmatrix} \tilde{\mathbf{y}}_N & \tilde{\mathbf{y}}_N^T \end{pmatrix} = \operatorname{diag}\begin{pmatrix} R_{\tilde{y}}(0) & R_{\tilde{y}}(1) & \cdots & R_{\tilde{y}}(N) \end{pmatrix}$$

Meanwhile,

$$\tilde{\mathbf{y}}_N = [\Omega_o \quad \Gamma_{w,o}] \begin{pmatrix} \tilde{\mathbf{s}}(0) \\ \bar{\mathbf{w}}_N \end{pmatrix}$$

leads to

$$\begin{aligned} &E\begin{pmatrix} \tilde{\mathbf{y}}_N & \tilde{\mathbf{y}}_N^T \end{pmatrix} \\ &= [\Omega_o \quad \Gamma_{w,o}] E\left( \begin{pmatrix} \tilde{\mathbf{s}}(0) \\ \bar{\mathbf{w}}_N \end{pmatrix} \begin{pmatrix} \tilde{\mathbf{s}}^T(0) & \bar{\mathbf{w}}_N^T \end{pmatrix} \right) \\ &\quad \cdot \begin{bmatrix} \Omega_o^T \\ \Gamma_{w,o}^T \end{bmatrix} \\ &= \begin{bmatrix} \Omega_o & \Gamma_{w,o} \end{bmatrix} I \begin{bmatrix} \Omega_o^T \\ \Gamma_{w,o}^T \end{bmatrix} = \Omega_o\Omega_o^T + \Gamma_{w,o}\Gamma_{w,o}^T. \end{aligned}$$

Then it can be concluded that

$$\begin{aligned} &W_{N,o}^T(\Omega_o\Omega_o^T + \Gamma_{w,o}\Gamma_{w,o}^T)W_{N,o} \\ &= W_{N,o}^T \operatorname{diag}(R_{\tilde{y}}(0) \quad R_{\tilde{y}}(1) \quad \cdots \quad R_{\tilde{y}}(N)))W_{N,o} \\ &= I. \end{aligned}$$

Therefore,

$$\|G_{rw}\|^2_{\infty,[0,N]} = \left\| \begin{array}{cc} W_N[\Omega & \Gamma_w] \end{array} \right\|_2^2 = 1.$$

*Stage 2*: Inspired by the analysis presented by Mangoubi (1998, p. 165), a new mapping from $r_{N,a}$ to $r_{N,o}$ in a more general sense is constructed in this paper. According to the FDF (7), $\tilde{y}(k)$ is a nonlinear function of $\{y(i)\}_{i=0}^k$. Therefore, there exists a nonlinear mapping $\mathcal{M}_y$ such that $\tilde{y}_N = \mathcal{M}_y y_N$. The converse is also true. For $k = 0$, $\hat{y}(0) = C\hat{x}_0$ is the estimate available prior to measurement $y(0)$, and we have $y(0) = \tilde{y}(0) + \hat{y}(0)$. For $k = 1$, $y(1) = \tilde{y}(1) + \hat{y}(1)$, where $\hat{y}(1)$ is a nonlinear function of $\tilde{y}(0)$ and the initial estimate. Hence $y(1)$ can be reconstructed from $\hat{x}_0$, $\tilde{y}(0)$ and $\tilde{y}(1)$. More generally, any $y(k)$ can be reconstructed from $\hat{x}_0$ and $\{\tilde{y}(i)\}_{i=0}^k$. Therefore, there exists a nonlinear mapping $\mathcal{M}_{\tilde{y}}$ such that $y_N = \mathcal{M}_{\tilde{y}}\tilde{y}_N$.

Therefore, a nonlinear mapping $\mathcal{M}_{ao}$ from $\tilde{y}_{N,o}$ to $\tilde{y}_{N,a}$ is constructed as $\tilde{y}_{N,a} = \mathcal{M}_y y_N = \mathcal{M}_y \circ \mathcal{M}_{\tilde{y}}\tilde{y}_{N,o} = \mathcal{M}_{ao}\tilde{y}_{N,o}$. Then

$$\begin{aligned} r_{N,a} &= W_{N,a}\tilde{y}_{N,a} = W_{N,a} \circ \mathcal{M}_{ao}\tilde{y}_{N,o} \\ &= W_{N,a} \circ \mathcal{M}_{ao} \circ W_{N,o}^{-1} W_{N,o} \\ &\quad (\Omega_o s(0) + \Gamma_{w,o}\bar{w}_N + \Gamma_{f,o} f_N) \\ &= \mathcal{H}_{rw} \begin{pmatrix} s(0) \\ \bar{w}_N \end{pmatrix} + \mathcal{H}_{rf}(f_N) \\ &= \mathcal{H}_{rr_o} \circ H_{rw,o} \begin{pmatrix} s(0) \\ \bar{w}_N \end{pmatrix} + \mathcal{H}_{rr_o} \circ H_{rf,o} f_N, \end{aligned}$$

where

$$\begin{aligned} \mathcal{H}_{rw} &= W_{N,a} \circ \mathcal{M}_{ao} \circ W_{N,o}^{-1} W_{N,o} \begin{bmatrix} \Omega_o & \Gamma_{w,o} \end{bmatrix}, \\ \mathcal{H}_{rf} &= W_{N,a} \circ \mathcal{M}_{ao} \circ W_{N,o}^{-1} W_{N,o} \Gamma_{f,o}, \\ \mathcal{H}_{rr_o} &= W_{N,a} \circ \mathcal{M}_{ao} \circ W_{N,o}^{-1}, \\ H_{rw,o} &= W_{N,o} \begin{bmatrix} \Omega_o & \Gamma_{w,o} \end{bmatrix}, \\ H_{rf,o} &= W_{N,o} \Gamma_{f,o}. \end{aligned}$$

**Remark 3.** Our analysis implies that output estimation errors contain all the information of measurements. Either output estimation errors or measurements can be recovered if the other one is known. Therefore, as long as the applied FDFs are stable, there always exist nonlinear mappings such that a residual sequence can be recovered from the other one.

*Stage 3*: For compatible nonlinear mapping $\mathcal{M}$ and matrix $H$, if $H$ satisfies $HH^T = I$, it can be obtained that $\|\mathcal{M} \circ H\|_\infty = \|\mathcal{M}\|_\infty$. Finally, we have

$$\begin{aligned} \frac{\|\mathcal{H}_{rf}\|_\infty^2}{\|\mathcal{H}_{rw}\|_\infty^2} &= \frac{\|\mathcal{H}_{rr_o} \circ H_{rf,o}\|_\infty^2}{\|\mathcal{H}_{rr_o} \circ H_{rd,o}\|_\infty^2} \\ &= \frac{\|\mathcal{H}_{rr_o} \circ H_{rf,o}\|_\infty^2}{\|\mathcal{H}_{rr_o}\|_\infty^2} \end{aligned}$$

$$\leq \frac{\|\mathcal{H}_{rr_o}\|_\infty^2 \|H_{rf,o}\|_2^2}{\|\mathcal{H}_{rr_o}\|_\infty^2}$$
$$= \|H_{rf,o}\|_2^2$$
$$= \frac{\|H_{rf,o}\|_2^2}{\|H_{rd,o}\|_2^2}$$

and

$$\frac{\|\mathcal{H}_{rf}\|_-^2}{\|\mathcal{H}_{rw}\|_\infty^2} = \frac{\|\mathcal{H}_{rr_o} \circ H_{rf,o}\|_-^2}{\|\mathcal{H}_{rr_o} \circ H_{rd,o}\|_\infty^2}$$
$$= \frac{\|\mathcal{H}_{rr_o} \circ H_{rf,o}\|_-^2}{\|\mathcal{H}_{rr_o}\|_\infty^2}$$
$$\leq \frac{\|\mathcal{H}_{rr_o}\|_\infty^2 \|H_{rf,o}\|_-^2}{\|\mathcal{H}_{rr_o}\|_\infty^2}$$
$$= \|H_{rf,o}\|_-^2$$
$$= \frac{\|H_{rf,o}\|_-^2}{\|H_{rd,o}\|_2^2}.$$

Based on the above analysis, the main result of this study is presented in the following proposition and algorithm.

**Proposition 1.** *For the nonlinear system (3) and its FDF (7), let matrices $A(k)$, $B_d(k)$, $B_w(k)$ and $\bar{A}(k)$, $\bar{C}(k)$, $\bar{K}(k)$, $\bar{B}_w(k)$, $\bar{D}_w(k)$ be defined by (15)–(18) and (20)–(25), respectively. When $\{\bar{A}(k), \bar{C}(k)\}$ is uniformly detectable and $\{\bar{A}(k), \bar{B}_w(k)\}$ is uniformly stabilizable, $K(k)$, $L(k)$ and $W(k)$ given in (26) constitute a suboptimal solution to (8) and (9). In this case, enhanced robust performance against multiple disturbances is achieved in the sense that compensation of $d(k)$ and optimization (8) and (9) are achieved simultaneously.*

**Algorithm 1.** Robust FDF based FD.

**Step 1.** Let $k = 0$, and set $\hat{x}(0) = \hat{x}_0$, $\hat{\zeta}(0) = 0$.

**Step 2.** Calculate the matrices $A(k)$, $B_d(k)$, $B_w(k)$ using (15), (16), (18), respectively, and construct the matrices $\bar{A}(k)$, $\bar{C}(k)$, $\bar{B}_w(k)$, $\bar{D}_w(k)$ according to (20), (21), (23), (24), respectively.

**Step 3.** Check whether or not $\{\bar{A}(k), \bar{C}(k)\}$ and $\{\bar{A}^T(k), \bar{B}_w^T(k)\}$ are detectable. If yes, go to Step 4, and stop the algorithm otherwise.

**Step 4.** Calculate $\bar{K}(k)$ and $W(k)$ using (26).

**Step 5.** Calculate $r(k)$ and $J_N(k)$ using (7) and (11), respectively, and trigger an alarm according to (13).

**Step 6.** A fault is declared at the time of $j_a$ as defined in (14).

**Step 7.** Calculate $\hat{x}(k+1)$ and $\hat{\zeta}(k+1)$ using (7).

**Step 8.** Let $k = k + 1$, go to Step 2 until the end of the process.

Table 1. Sensor noise characteristics for simulation.

| | $V_m$ | $q_m$ | $\theta_m$ | $H_m$ |
|---|---|---|---|---|
| $\sigma$ | 0.2 m/s | 0.05 rad/s | 0.05 rad | 3 m |

## 4. Simulation study

In this section, both simulations and real flight data are applied to validate the proposed method. Simulations with a nonlinear UAV model are carried out in the MATLAB/Simulink environment. All model parameters are obtained for a real UAV and the aerodynamic coefficients are obtained from a wind tunnel test. Noise characteristic of the measurements are given in Table 1, where $\sigma$ stands for the standard deviation of measurement noise. A flight in gusty conditions is considered. The well-known Dryden model is used to generate turbulence, while the gust is simulated as superposition of parts of sine waves in $W_z$. Wind speeds in the horizontal and vertical directions are depicted in Fig. 1.

In addition, in appreciation of the remarkable work of the UAV research group of the University of Minnesota, real flight data of a small UAV named 'Thor' is also employed in this study. More details about the UAV platform and the open source of raw data, mathematical models, and simulations can be found at `http://www.uav.aem.umn.edu/`. Since flight data of an elevator fault or a throttle fault are unavailable, a piece of fault free data is employed and scenarios of sensor faults are simulated by adding artificial signals to the original measurements. The states and the position trajectory of the UAV 'Thor' of the applied data are demonstrated in Fig. 2.

Four different fault scenarios are considered. Scenarios of actuator faults are considered in computer simulations, while flight data of the 'Thor' are employed to simulate sensor faults. Details about these fault

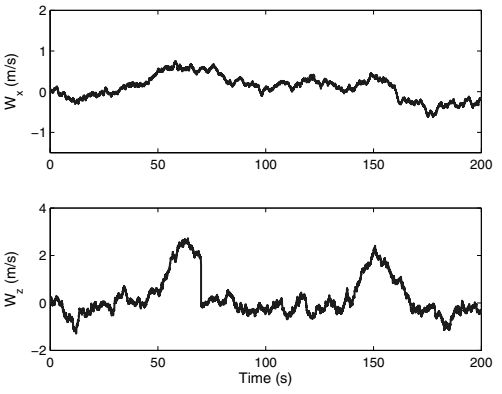


Fig. 1. Wind speed in simulation.

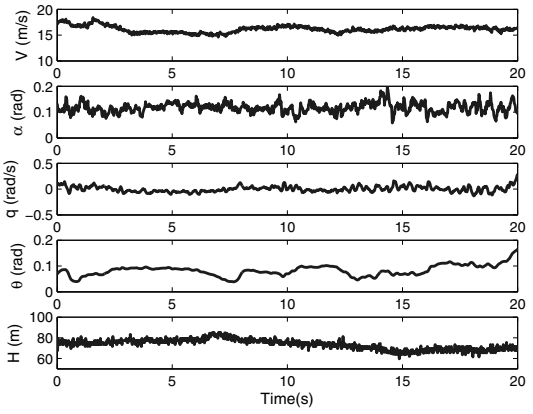


(a)

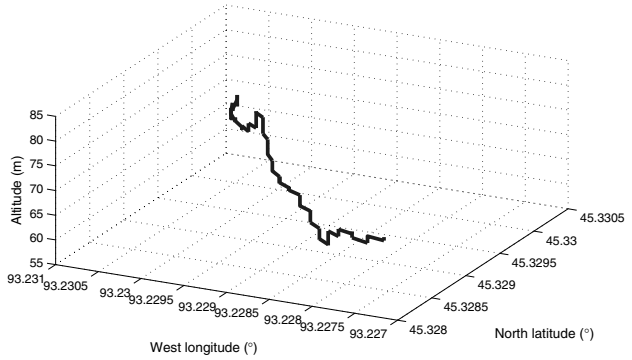


(b)

Fig. 2. Flight data of the UAV 'Thor': longitudinal states (a), position trajectory (b).

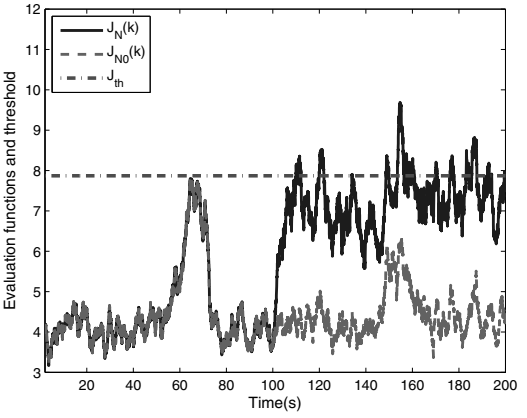


(a)

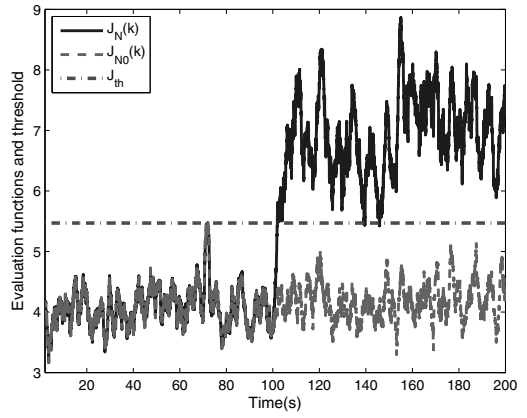


(b)

Fig. 3. FD results for elevator fault: by extended $H_-/H_\infty$-FDF (a), by the FDF (7) (b).

scenarios are presented as follows:

- In Scenario I, computer simulation is adopted. The bias of the elevator from its desired position is considered, and the fault is modeled as $\delta_{e,f}(t) = \delta_{e,o}(t) + 1^\circ$ when $t > 100$ s.
- In Scenario II, computer simulation is adopted. A loss of effectiveness of the throttle is considered, and the fault is modeled as $\delta_{p,f}(t) = 0.6 \cdot \delta_{p,o}(t)$ when $t > 100$ s.
- In Scenario III, flight data are employed. An intermittent fault of the pitot is considered, and the fault is modeled as $V_{m,f}(t) = 1.2V_{m,o}(t)$ when $10\,\text{s} \le t \le 12\,\text{s}$, $14\,\text{s} \le t \le 16\,\text{s}$ and $18\,\text{s} \le t \le 20\,\text{s}$.
- In Scenario IV, flight data is employed. Drift of the rate gyro is considered, and the fault is modeled as $q_{m,f}(t) = q_{m,o}(t) + 0.05(t - 10)$ rad/s when $10\,\text{s} \le t < 12\,\text{s}$ and $q_{m,f}(t) = q_{m,o}(t) + 0.1$ rad/s when $t \ge 12\,\text{s}$.

In the above fault models, the subscripts $f$ and $o$ indicate the faulty value and the nominal value, respectively.

To show the advantage of the proposed method in handling multiple disturbances, the extended $H_-/H_\infty$-FDF proposed by Zhong *et al.* (2015) is also applied for FD. A sliding window with $N = 100$ is employed, and the threshold is chosen as

$$J_{th} = \sup_{\bar{w}(k)} J_{N0}(k),$$

where $J_{N0}(k)$ is $J_N(k)$ in the fault-free case. Detection performance of these scenarios is demonstrated as follows.

FD results of Scenario I are shown in Fig. 3. It can be observed in Fig. 3(a) that the elevator fault is hardly detectable when the extended $H_-/H_\infty$-FDF is used. In Fig. 3(b), the elevator fault is detected successfully because of a lower threshold result from wind estimation and compensation. Similar FD performance of Scenario II is depicted in Fig. 4.

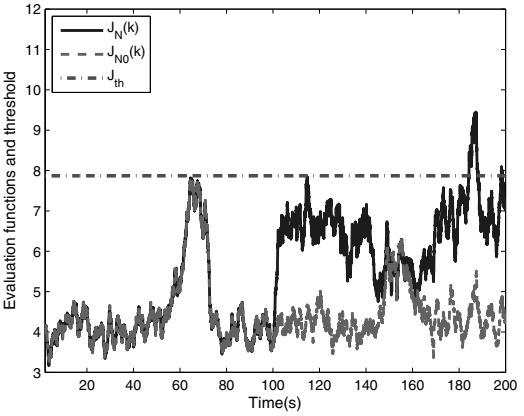


(a)

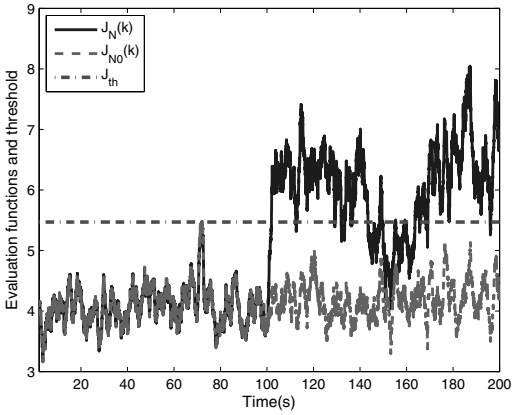


(b)

Fig. 4. FD results for the throttle fault: by extended $H_-/H_\infty$-FDF (a), by the FDF (7) (b).

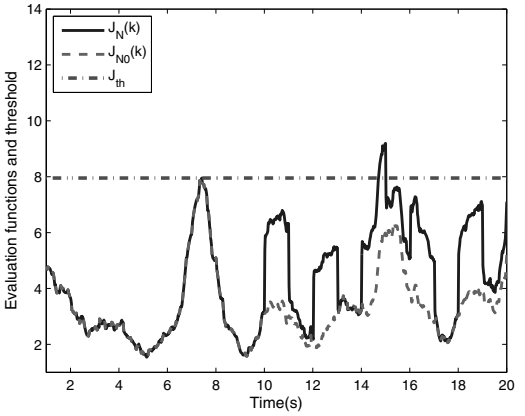


(a)

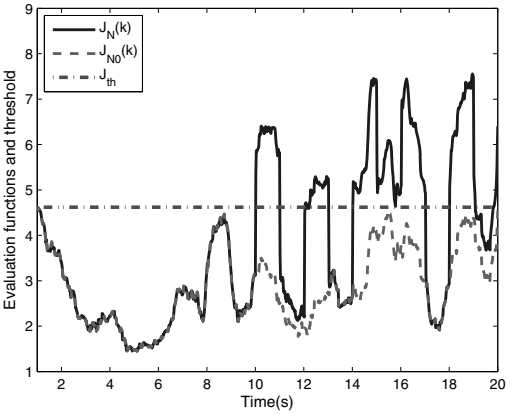


(b)

Fig. 5. FD results for the pitot fault: by extended $H_-/H_\infty$-FDF (a), by the FDF (7) (b).

When flight data are employed, FD results of Scenarios III and IV are shown in Figs. 5 and 6, respectively. As is illustrated in Fig. 5(a), the intermittent pitot fault is undetectable for most of the time when the conventional $H_-/H_\infty$-FDF is used. A much better FD performance is achieved by the proposed FDF (7), as depicted in Fig. 5(b). When the gyro fault in Scenario IV is considered, it is shown in Fig. 6 that it takes a considerable time to detect the fault after its occurrence when the extended $H_-/H_\infty$-FDF is used. On the contrary, the proposed FDF (7) accomplish the detection task much faster.

## 5. Conclusion

In this paper, FD of actuator and sensor faults for the UAV FCS has been investigated. In order to cope with multiple sources of disturbances including wind effects, modeling errors and sensor noises, a disturbance estimation and compensation procedure is integrated into $H_i/H_\infty$-FDF design and the detection performance is improved. On the other hand, future works need to be carried out to make this investigation more complete. For example, the observability condition of the disturbance $d(k)$ should be identified. Though conditions for reconstructibility of unknown inputs for linear time invariant systems have been presented in the work of Ding (2013) and the references therein, the problem becomes much more difficult for nonlinear time varying systems. In addition, fault isolation, fault estimation and their applications with fault tolerant control are further problems with great interest and challenges, and these would be topics of our future studies.

## Acknowledgment

This work is partially supported by the National Natural Science Foundation of China (grants no. 61333005, 61733009, 61673032) and the Research Fund for the Taishan Scholar Project of the Shandong Province of China.

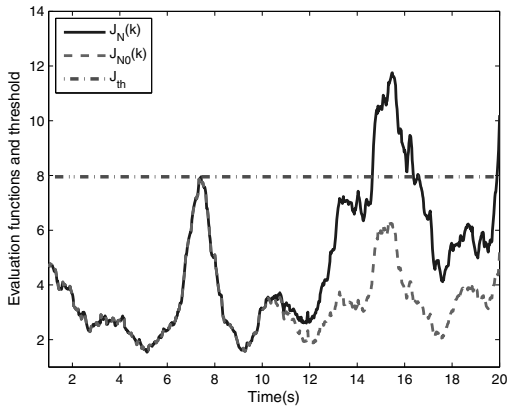


(a)

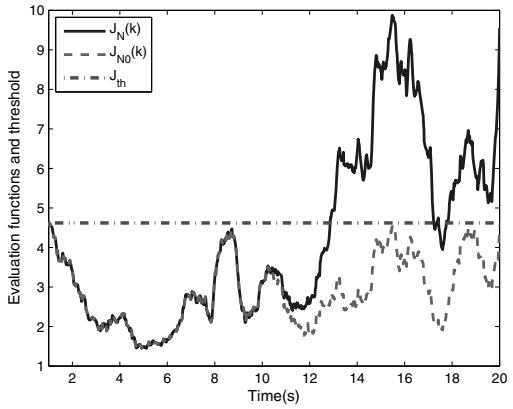


(b)

Fig. 6. FD results of gyro fault: by extended $H_-/H_\infty$-FDF (a), by the FDF (7) (b).

## References


Bateman, F., Noura, H. and Ouladsine, M. (2011). Fault diagnosis and fault-tolerant control strategy for the aerosonde UAV, *IEEE Transactions on Aerospace and Electronic Systems* **47**(3): 2119–2137.

Boulkroune, B., Halabi, S. and Zemouche, A. (2013). $H_-/H_\infty$ fault detection filter for a class of nonlinear descriptor systems, *International Journal of Control* **86**(2): 253–262.

Caliskan, F., Zhang, Y., Wu, N.E. and Shin, J.Y. (2014). Actuator fault diagnosis in a Boeing 747 model via adaptive modified two-stage Kalman filter, *International Journal of Aerospace Engineering* **2014**: 1–10.

Cen, Z., Noura, H. and Younes, Y.A. (2015). Systematic fault tolerant control based on adaptive Thau observer estimation for quadrotor UAVs, *International Journal of Applied Mathematics and Computer Science* **25**(1): 159–174, DOI: 10.1515/amcs-2015-0012.

Chabir, K., Sid, M.A. and Sauter, D. (2014). Fault diagnosis in a networked control system under communication constraints: A quadrotor application, *International Journal of Applied Mathematics and Computer Science* **24**(4): 809–820, DOI: 10.2478/amcs-2014-0060.

Cho, A., Kim, J., Lee, S. and Kee, C. (2011). Wind estimation and airspeed calibration using an UAV with a single-antenna GPS receiver and pitot tube, *IEEE Transactions on Aerospace and Electronic Systmes* **47**(1): 109–117.

Ding, S.X. (2013). *Model-Based Fault Diagnosis Techniques: Design Schemes, Algorithms, and Tools*, Springer, Berlin.

Ding, S.X., Jeinsch, T., Frank, P.M. and Ding, E.L. (2000). A unified approach to the optimization of fault detection systems, *International Journal of Adaptive Control and Signal Processing* **14**(7): 725–745.

Ducard, G. and Geering, H.P. (2008). Efficient nonlinear actuator fault detection and isolation system for unmanned aerial vehicles, *Journal of Guidance, Control, and Dynamics* **31**(1): 225–237.

Freeman, P., Pandita, R., Srivastava, N. and Balas, G.J. (2013). Model-based and data-driven fault detection performance for a small UAV, *IEEE/ASME Transactions on Mechatronics* **18**(4): 1300–1309.

Frost, W. and Bowles, R.L. (1984). Wind shear terms in the equations of aircraft motion, *Journal of Aircraft* **21**(11): 866–872.

Guo, L. and Cao, S. (2014). Anti-disturbance control theory for systems with multiple disturbances: A survey, *ISA Transactions* **53**(4): 846–849.

Hajiyev, C. (2013). Two-stage Kalman filter-based actuator/surface fault identification and reconfigurable control applied to F-16 fighter dynamics, *International Journal of Adaptive Control and Signal Processing* **27**(9): 755–770.

Hassanabadi, A.H., Shafiee, M. and Puig, V. (2016). Robust fault detection of singular LPV systems with multiple time-varying delays, *International Journal of Applied Mathematics and Computer Science* **26**(1): 45–61, DOI: 10.1515/amcs-2016-0004.

Henry, D., Cieslak, J., Zolghadri, A. and Efimov, D. (2015). $H_\infty/H_-$ LPV solutions for fault detection of aircraft actuator faults: Bridging the gap between theory and practice, *International Journal of Robust and Nonlinear Control* **25**(5): 649–672.

Khan, A.Q., Abid, M. and Ding, S.X. (2014). Fault detection filter design for discrete-time nonlinear systems—A mixed $H_-/H_\infty$ optimization, *Systems & Control Letters* **67**(1): 46–54.

Langelaan, J.W., Alley, N. and Neidhoefer, J. (2011). Wind field estimation for small unmanned aerial vehicles, *Journal of Guidance, Control, and Dynamics* **34**(4): 1016–1030.

Lee, J.H., Sevil, H.E., Dogan, A. and Hullender, D. (2014). Estimation of receiver aircraft states and wind vectors in aerial refueling, *Journal of Guidance, Control, and Dynamics* **37**(1): 265–276.

Li, X., Liu, H.H.T. and Jiang, B. (2015). Parametrization of optimal fault detection filters, *Automatica* **56**: 70–77.

Lu, P., Eykeren, L.V., Kampen, E.V. and Chu, Q.P. (2015). Selective-reinitialization multiple-model adaptive estimation for fault detection and diagnosis, *Journal of Guidance, Control, and Dynamics* **38**(8): 1409–1424.

Lu, P., Kampen, E.V., Visser, C.D. and Chu, Q.P. (2016). Nonlinear aircraft sensor fault reconstruction in the presence of disturbances validated by realflight data, *Control Engineering Practice* **49**: 112–128.

Mangoubi, R.S. (1998). *Robust Estimation and Failure Detection: A Concise Treatment*, Springer, London.

Mulgund, S.S. and Stengels, R.F. (1996). Optimal nonlinear estimation for aircraft flight control in wind shear, *Automatica* **32**(1): 3–13.

Nicotra, M.M., Naldi, R. and Garone, E. (2017). Nonlinear control of a tethered UAV: The taut cable case, *Automatica* **78**: 174–184.

Péni, T., Vanek, B., Szabó, Z. and Bokor, J. (2015). Supervisory fault tolerant control of the GTM UAV using LPV methods, *International Journal of Applied Mathematics and Computer Science* **25**(1): 117–131, DOI: 10.1515/amcs-2015-0009.

Pereira, P.O., Cunha, R., Cabecinhas, D., Silvestre, C. and Oliveira, P. (2017). Leader following trajectory planning: A trailer-like approach, *Automatica* **75**: 77–87.

Rodriguez-Alfaro, L.H., Alcorta-Garcia, E., Lara, D. and Romero, G. (2015). A Hamiltonian approach to fault isolation in a planar vertical take-off and landing aircraft model, *International Journal of Applied Mathematics and Computer Science* **25**(1): 65–76, DOI: 10.1515/amcs-2015-0005.

Rosa, P. and Silvestre, C. (2013). Fault detection and isolation of LPV systems using set-valued observers: An application to a fixed-wing aircraft, *Control Engineering Practice* **21**(3): 242–252.

Tanaka, N. and Suzuki, S. (2006). Restructurable guidance and control for aircraft with failures considering gust effects, *Journal of Guidance, Control, and Dynamics* **29**(3): 671–679.

University of Minnesota (2012). UAV research group, University of Minnesota, Minneapolis, MN, `http://www.uav.aem.umn.edu/`.

Wu, C., Qi, J., Song, D., Qi, X. and Han, J. (2015). Simultaneous state and parameter estimation based actuator fault detection and diagnosis for an unmanned helicopter, *International Journal of Applied Mathematics and Computer Science* **25**(1): 175–187, DOI: 10.1515/amcs-2015-0013.

Xu, F., Puig, V., Ocampo-Martinez, C., Olaru, S. and Niculescu, S.-I. (2017). Robust MPC for actuator fault tolerance using set-based passive fault detection and active fault isolation, *International Journal of Applied Mathematics and Computer Science* **27**(1): 43–61, DOI: 10.1515/amcs-2017-0004.

Zhao, S. and Huang, B. (2017). Iterative residual generator for fault detection with linear time-invariant state-space models, *IEEE Transactions on Automatic Control* **62**(10): 5422–5428.

Zhong, M., Ding, S.X. and Ding, E.L. (2010). Optimal fault detection for linear discrete time-varying systems, *Automatica* **46**(8): 1395–1400.

Zhong, M., Ding, S.X. and Zhou, D. (2016a). A new scheme of fault detection for linear discrete time-varying systems, *IEEE Transactions on Automatic Control* **61**(9): 2597–2602.

Zhong, M., Guo, J., Guo, D. and Yang, Z. (2016b). An extended $H_i/H_\infty$ optimization approach to fault detection of INS/GPS-Integrated system, *IEEE Transactions on Instrumentation and Measurement* **65**(11): 2495–2504.

Zhong, M., Liu, H. and Song, N.F. (2015). On designing an extended $H_-/H_\infty$-FDF for a class of nonlinear systems, *Proceedings of the 9th IFAC Symposium on Fault Detection, Supervision and Safety for Technical Processes SAFEPROCESS 2015, Paris, France*, pp. 707–712.

Zhong, M., Zhang, L., Ding, S.X. and Zhou, D. (2017). A probabilistic approach to robust fault detection for a class of nonlinear systems, *IEEE Transactions on Industrial Electronics* **64**(5): 3930–3939.

**Hai Liu** received the BE degree from the College of Engineering, Zhejiang Normal University, China, in 2010, and the ME degree from the School of Traffic and Transportation, Beijing Jiaotong University, China, in 2013. He is currently a PhD student at the Department of Inertia Technology and Navigation Instrumentation, Beihang University, Beijing. His research interests are model-based fault diagnosis and applications.

**Maiying Zhong** received the PhD degree in control theory and control engineering from Northeastern University, Shenyang, China, in 1999. From 2002 to July 2008, she was a professor in the School of Control Science and Engineering, Shandong University. From 2006 to 2007, she was a postdoctoral researcher fellow with the Central Queensland University, Australia. From 2009 to 2016, she was a professor in the School of Instrument Science and Opto-Electronics Engineering, Beihang University. In 2016, she joined the Shandong University of Science and Technology, Qingdao, China, where she is currently a professor in the College of Electrical Engineering and Automation. Her research interests include model-based fault-diagnosis, fault-tolerant systems, and their applications.

**Rui Yang** received the BEng in computer engineering and a PhD in electrical engineering from the National University of Singapore, in 2008 and 2013, respectively. He is currently a lecturer in the College of Electrical Engineering and Automation of the Shandong University of Science and Technology. His research interests include fault diagnosis and precision motion control.

Received: 19 June 2017
Revised: 23 November 2017
Re-revised: 17 January 2018
Accepted: 28 January 2018